

Interstitial Boron-doped TiO₂ thin films: the significant effect of boron on TiO₂ coatings grown by atmospheric pressure chemical vapour deposition

Miguel Quesada-González,^{†‡} Nicolas D. Boscher,[‡] Claire J. Carmalt[†] and Ivan P. Parkin^{†}*

[†] Materials Chemistry Research Centre, Department of Chemistry, University College London, 20 Gordon Street, London WC1H 0AJ, United Kingdom.

[‡] Department of Materials Research and Technology, Luxembourg Institute of Science and Technology, 5 Avenue des Hauts-Fourneaux, Esch-sur-Alzette, L-4362, Luxembourg.

KEYWORDS: Atmospheric pressure chemical vapour deposition (APCVD), interstitial boron-doped TiO₂, enhancement of average crystal size, photoactive thin films.

ABSTRACT: The work presented here describes the preparation of transparent interstitial boron-doped TiO₂ thin-films by atmospheric pressure chemical vapour deposition (APCVD). The interstitial boron-doping, on TiO₂, proved by X-ray photoelectron spectroscopy (XPS) and X-ray diffraction (XRD), is shown to enhance the crystallinity and significantly improve the photocatalytic activity of the TiO₂ films. The synthesis, highly suitable for a reel-to-reel process, has been carried out in one step.

Titanium dioxide (TiO₂) thin films have been extensively studied due to their multifunctional applications and physical possibilities.¹ The capability of TiO₂ to photoactivate various reactions, its chemical inertness, lifetime and the fact that it is easily synthesised and deposited by simple chemical processes,² has prevailed it a global interest in several applications,³ including water and air purification, antibacterial coating,⁴ self-cleaning materials,⁵ photoelectrochemical cells for solar energy harvesting devices,⁶ electricity production and water splitting.⁷ The main field of research has predominantly emphasized titania in the oxidation of organic pollutants,⁸ a field which has led to the industrial use of TiO₂ for the production of environmental, self-cleaning and photocatalytic technologies such as the Pilkington Activ™ Glass.⁹

The reported methods of synthesis which can be used for the formation of TiO₂ thin films include the sol-gel method,¹⁰ hydrothermal method,¹¹ surface impregnation, electrochemical deposition,¹² physical¹³ and chemical vapour deposition methods.¹⁴ Chemical vapour deposition (CVD), and most particularly atmospheric-pressure CVD (APCVD) of TiO₂ presents some advantages when compared to other routes such as sol-gel, since a calcination or annealing step is not required to obtain the crystalline anatase and/or rutile phases.¹⁵ The annealing process can affect drastically the nature and content of the dopant.¹⁶ In general terms, CVD processes offer the widest range of thin film and coating applications than any other deposition or coating techniques, making them easy to scale to a reel-to-reel process.¹⁷

Many solutions have been studied in order to improve the photocatalytic properties of TiO₂. The combination of anatase TiO₂ with its rutile phase¹⁸ or with other materials, such as noble metals nanoparticles¹⁹ can significantly enhance the photocatalytic properties of TiO₂. Doping of

TiO₂ with foreign elements, metal or non-metal, can also enhance the performances of TiO₂ through a narrowing of the band gap or by creating defect levels within the band gap.²⁰ Non-metal or anion dopants do not cause major narrowing of the band gap, yet these impurity states participate in trapping the charges to cause improvement in the photocatalytic activity.²¹ Boron doping of TiO₂ has attracted attention due to its inductive creation of electron acceptor levels.²² When boron is doped into the TiO₂ lattice, boron atoms can occupy two different positions, an interstitial position and a substitutional position by filling up the oxygen vacancies.²³ When boron occupies an interstitial position within the TiO₂ lattice, the stability of the doped TiO₂ is far better when compared to the substitutional boron, which appear to be metastable and decompose into boron oxide.²⁴ Previously, the synthesis of boron-doped TiO₂ has been focused on the formation of powders by sol-gel, annealing and hydrothermal methods.²⁵ Recently, B-TiO₂ thin films deposited by APCVD have been reported for the first time by Carmichael *et al.*²⁶ The boron dopant, incorporated in an O-substitutional position into the TiO₂, did lead to remarkable rates of hydrogen production and more favourable photocurrent profiles when compared to non-doped samples.

In this work, interstitial boron-doped TiO₂ thin-films were grown by APCVD on a float glass substrate. The interstitial boron dopant provided to B-TiO₂ transparent thin-films an improved photocatalytic performance, as well as an increase of the particle crystallite size, compared to undoped TiO₂ thin-films. The deposition of the films was carried out by controlling the vapour pressure of the boron source, boron isopropoxide (B[(CH₃)₂CHO]₃), by heating up the stainless steel bubbler to 364 K. The temperature and mass flow values were constant for metal (TiCl₄) and oxygen (CH₃COOC₂H₅) precursors; 340 K and 310 K and 6.4×10^{-3} and 3.04×10^{-3} g·min⁻¹, respectively. The heated precursors were carried to 2 mixing chambers by using N₂ as the carrier

gas. The mixing chamber containing O and Ti precursors, was kept at a constant temperature of 523 K, whereas the mixing chamber containing the boron precursor, was kept at 473K. The glass substrate was placed in the reactor and heated up to 773 K, when the deposition took place.

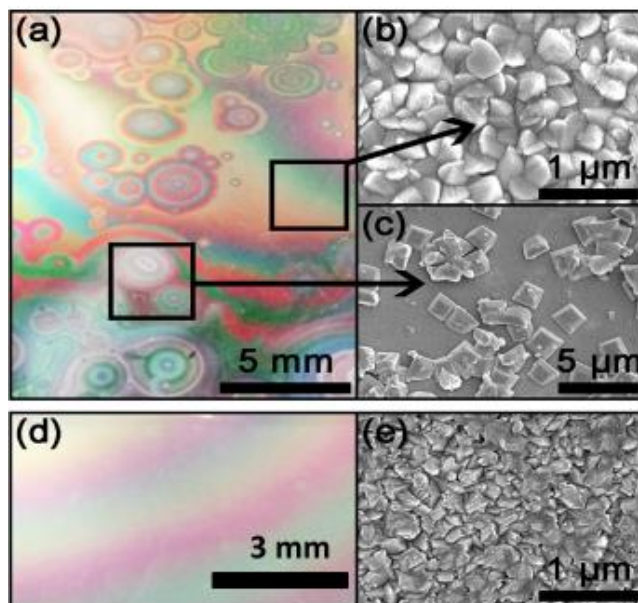


Figure 1. (a) Optical image with a tilt angle of the B-TiO₂ thin film on glass and (b and c) the corresponding SEM images from two different areas identified on the B-TiO₂ thin film, and (d) optical image of the undoped TiO₂ and (e) its SEM capture.

Both, the undoped and boron-doped TiO₂ thin films described in this work were relatively hard and strongly adherent across the whole length of the glass substrate (see Fig. S1a & b).

Preliminary visual observations under tilt angle showed undoubted different surfaces morphologies between the films (Figure 1a & d). The undoped TiO₂ coating exhibits different lines of interference colours, expressing thickness differences along the length of the substrate (Fig. 1d). On the other hand, a combination of these lines and concentric circles of interference colours were observed on the B-TiO₂ thin film (Figure 1a). SEM observations confirm the

existence of morphology discrepancies between the B-TiO₂ (Figure 1b & c) and TiO₂ coatings (Figure 1e). In addition, SEM analyses of the B-TiO₂ sample revealed the presence of two different morphologies, which correspond to the macroscopic aspect variation shown in Figure 1a. Figure 1b shows prism-shaped and well aggregated particles with sizes in the range of 290 to 500 nm, whereas the agglomerations of bigger particles (ca. 1 μm to 2.3 μm) with a more defined prism-like and cubic shape, deposited on top of a uniform coating with smaller agglomerations of particles, were observed in the concentric circles zones (Figure 1c). When comparing the two different surface morphologies identified on the boron-doped TiO₂ film (Figure 1b & c) with the surface morphology of the undoped TiO₂ film (Figure 1e) deposited under the same conditions, the effect of the addition of the boron precursor on the morphology of the films is obvious. Indeed, the typical SEM image of the TiO₂ film shows shell-shaped aggregated particles with sizes in the range from 120 to 230 nm, which contrasts with the significantly larger average particle size of the B-TiO₂ sample (i.e. 290 to 500 nm). The formation of concentric circles might be explained due to zones where the gas phase reaction between precursors was prevailing along the glass substrate (89 × 225 × 4mm) and the 3D growth of clusters is promoted as the reaction take place more in the gas phase than directly on top of the substrate (2D growth).

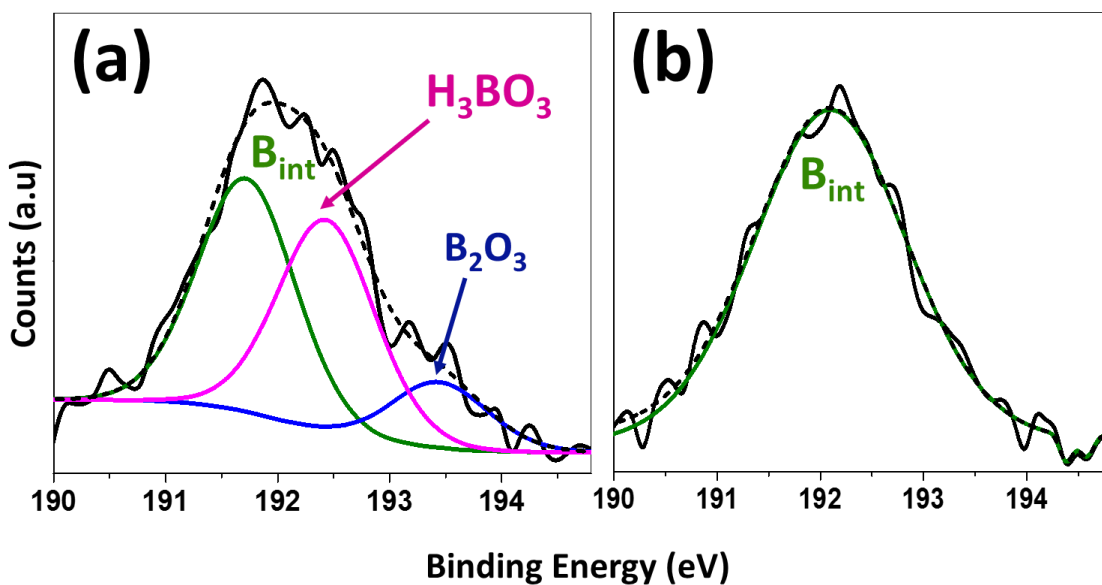


Figure 2. XPS spectra of B 1s in the B-TiO₂ film. Surface spectrum (a) and bulk spectrum (b) obtained by in-depth profiling. Envelope represented by the dashed black line.

To evidence the presence of boron in the films and elucidate its position in the film or within the TiO₂ lattice, XPS analyses were performed both on the surface of the film and in depth. The Ti 2p peaks, located at binding energies of 458.9 and 464.6 eV, were identified as Ti-O bonds of Ti⁴⁺ in TiO₂.²⁷ No other Ti⁴⁺ environment or reduced Ti³⁺ species were detected (see figure S2). The O 1s peak located at 530.4 eV, is also consistent with the formation of TiO₂.²⁴ The boron concentration on the surface of the film was found to be in the range of 5-6 at. %. Regarding the chemical environment of boron in boron-containing TiO₂, many discrepancies can be found in the literature. First, boron can be embedded either as a substitutional or interstitial dopant in the TiO₂ lattice. Generally, B 1s peaks at 190–191 eV are attributed to boron in an oxygen substitutional position and peaks in the range 191–192 eV to interstitial boron.²⁸ Boron can also be found in various other forms, including cationic B³⁺ in B₂O₃ and anionic B²⁻ in TiB₂, with a characteristic

B 1s peak lying at 193.1 and 187.5 eV, respectively.^{24,28} In addition, a peak at 192.6 eV can be attributed to H₃BO₃ or B₂O₃. From Figure 2a, it can be observed that after deconvolution of the B 1s peak obtained from the XPS surface analysis of the B-TiO₂ film, three peaks are allocated. The main one, located at 192 eV, suggests that boron occupies an interstitial position in the TiO₂ lattice. The two other peaks, with much lower intensities, located at 192.6 and 193.3 eV, are attributed to H₃BO₃ and B₂O₃, respectively. The in-depth XPS spectrum (Figure 2b), showed after deconvolution only one component, located at 191.7 eV, attributed to the interstitial boron. It can be concluded that the species H₃BO₃ and B₂O₃ are only present on the surface of the films, and they may appear due to the reaction process in the gas phase, as by-products.

XRD analysis of the B-TiO₂ sample, which indicates the formation of anatase TiO₂, is also suggesting an interstitial doping of the boron element. Indeed, the lattice parameters of the B-TiO₂, calculated from the XRD data fitted with the Le Bail method, were shown to be larger than the ones of the reference TiO₂ sample (Figure 3a).

(a) Sample	A[Å]	C[Å]	V[Å] ³	τ [nm]
TiO ₂	3,7885	9,5205	136,6477	45
B _{int} -TiO ₂	3,7832	9,5361	137,7203	87
B _{sub} -TiO ₂ ^[26]	3,7871	9,4844	136,0264	20

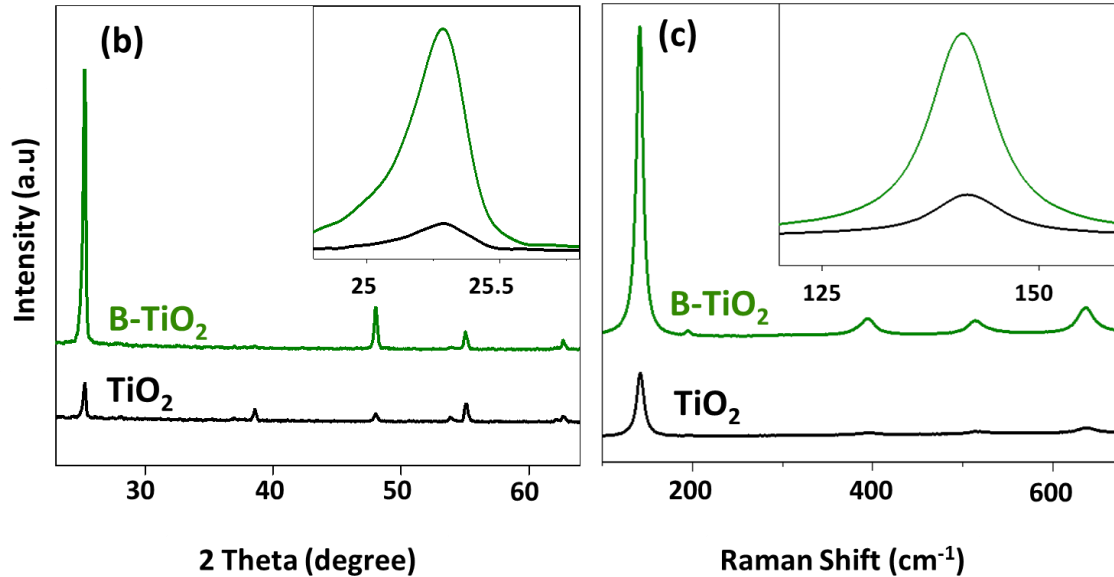


Figure 3. (a) Table containing the cell parameters of undoped and both boron-doped TiO₂, interstitial and substitutional, synthesised under the same conditions; (b) XRD pattern and (c) Raman spectrum of both films compared, both with an inset focused on the main peak for anatase.

The extension of the c-axis and the expansion of the unit cell volume can be explained by the interstitial incorporation of boron in the TiO₂ lattice. This interstitial occupation of boron within the lattice, differs from the previous APCVD work done by Carmichael *et al.*,²⁶ where boron was found to occupy an O-substitutional position such as assumed from the contraction of the c-axis of the unit cell. When comparing parameters of the deposition by APCVD, the critical parameters to obtain substitutional rather than interstitial boron, as well as a more powdery

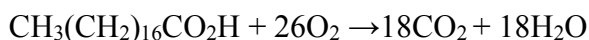
coating in contrast to an adherent thin film, are the temperature of the bubbler where triisopropyl borate is located, the temperature of the mixing chamber and the flow rate of the precursors. In this work, the temperature of the triisopropyl borate bubbler was higher (90 °C vs 75°C), so the generated vapour pressure was higher. However, the temperature of the mixing chamber, where the boron precursor is kept just before the reaction takes place, was lower (200°C vs 250°C) and a decreased flow rate of the dopant precursor was used (0.1 L/min vs 0.5 L/min). A lower temperature for the mixing chamber and decreased flow rate allows more time for the species to react in the gas phase and hence results in the formation of interstitial-doped boron TiO₂ rather than substitutional-doped boron TiO₂. The interstitial incorporation of boron within TiO₂ presents some advantages compared to the O-substitutional sites occupied for such element, demonstrated by Artiglia et al.²⁸ It was reported that when annealing, the substitutional sites of B disappear to form B₂O₃ while the interstitial B is highly stable at all temperatures, suggesting that interstitial boron is the preferred and the most stable site in TiO₂. To prove the stability of the interstitial B, thermal treatment of synthesized B-TiO₂ thin film at atmospheric pressure was performed in the AnnealSys furnace. The annealing program, comprising of a heating rate of 5 °C per minute rise to 500 °C, 4 hours stay at the temperature and cooling down to RT.

The XPS analysis of the sample after sintering showed still the presence of interstitial B (≈ 3% at.) in the surface (see SI, Fig. S2c). Additionally, interstitial boron decreases the recombination process, trapping electrons and perpetuating the lifetime of the charge carriers (holes and electrons). Furthermore, previous calculations by DFT, suggested better mobility and low recombination rate for interstitial B-TiO₂.²⁵

Another significant distinction from the work by Carmichael et al. is the crystallinity enhancement of the TiO₂ thin film when doped with interstitial boron. While, O-substitutional

boron-doping of APCVD TiO₂ was reported to imply a crystallinity devaluation²⁶ (i.e. crystallite sizes reduced by a factor 2), both the Raman and XRD spectra of the B-TiO₂ film elaborated in this work showed anatase peaks of greater intensities when compared to the undoped TiO₂ films (Figure 3a). The crystallite sizes, related to the intensity and shape of the peaks recorded by XRD and Raman, were nearly doubled when employing the boron precursor (i.e. 45 and 87 nm for the TiO₂ and B-TiO₂ coatings, respectively). This finding is also supported by the SEM observations (Figure 1b & e), which sustain a higher crystallinity of the B-TiO₂ thin film. It is also worth noting that the morphology of the B-TiO₂ thin film described herein were significantly different to the films reported by Carmichael *et al.*, where elongated and blade-like structure of the doped films were observed.²⁶

The increased crystallinity of the B-TiO₂ sample may contribute to superior functional properties of the film in comparison to undoped TiO₂.^{21,24} To investigate the influence of interstitial boron doping on one of the functional properties of TiO₂, a photocatalytic activity test of the B-TiO₂ films was performed and evaluated by the degradation of stearic acid under UVA irradiation (1.2 mW·cm⁻²). The photocatalytic reaction is given by the equation:



The photocatalytic process was recorded using FTIR (see Fig. S3), following the disappearance of characteristic C–H vibrational modes of the stearic acid (2958, 2923 and 2853 cm⁻¹). The photocatalytic rates were estimated from linear regression of the initial steps (30–40%) of the curve of integrated area versus illumination time.²⁹ The corresponding rates were expressed as formal quantum efficiencies (FQE), defined as molecules of stearic acid degraded over incident photons (units, molecule·photon⁻¹) (Figure 4a). The photoactivity of the

B-TiO₂ film (Figure 4a) was enhanced when compared to the undoped films deposited under the same conditions. For the first run, the FQE of B-TiO₂ was found to be 9 times higher compared to the average FQE calculated for undoped TiO₂ films. After the first run of photocatalysis, the performance of the B-TiO₂ thin film decreases compared to the first run of the photocatalytic test, however, the performance of the boron-doped TiO₂ films is superior to the average performance of the undoped films (Figure 4a, B-TiO₂ bars 2,3 and 4). The superior photocatalytic activities of the B-TiO₂ thin film could be correlated directly with both the enhanced crystallinity of the films and the presence of boron in the TiO₂ lattice. Indeed, the incorporation of boron induces a change in the morphology and significantly increases the average crystallite size, so reduces the rate of photoexcited e⁻/h⁺ recombination. In addition, boron-doping is known to induce a narrowing of the band gap.²⁵ UV-Visible spectrophotometry of the films was selected to determine the experimental optical band gap of B-TiO₂. Compared to the undoped TiO₂, after the determination of the band gap by Tauc plot, only a small difference in energy was appreciated, 3.3 eV for undoped TiO₂ and 3.28 for B-TiO₂. The transmittance spectra of the films (see figure S5) showed a small shift in absorption into the blue region for B-TiO₂. To evidence the shifting of the valence band maximum (VBM), VB-XPS analysis was performed (Figure 4b). As it can be seen in figure 4b, there is a small shift when comparing B-TiO₂ VBM to the undoped TiO₂. Although there is not a big change observed in energy, XPS analysis confirms that upon the addition of B to the TiO₂ lattice, interband states are formed and added between the conduction and valence bands of TiO₂. These interband states will most likely be close to the valence band of TiO₂, interacting with the O 2p orbitals of the TiO₂ valence band.

To test and demonstrate the stability and permanence of the dopant (i.e. boron) within the TiO₂ structure when incorporated in the interstitial position, analysis by XPS was carried out for the B-TiO₂ sample over the same area before and after the photocatalytic test. XPS surface analysis shows a stable concentration of boron (ca. 5 at. %) in the coating surface, even after the cleaning step with chloroform and after UV light (365nm) irradiation for a period of 48 h and after three repetitions of the photocatalytic test (Figure 4c & d). In addition, the core-level B 1s XPS spectrum (Figure 4c & d) revealed, after deconvolution, a dominant peak at 191.7 eV, which corresponds to the interstitial boron (between 191-192 eV). When comparing to the core-level B 1s XPS spectrum prior to the photocatalytic test (Figure 2a), it can be notice that the peak assigned to B₂O₃ disappeared completely and the peak attributed to H₃BO₃ decreased its intensity and area. Both species, present in the surface of the film, were probably dissolved at some point when irradiating or cleaning the sample. The XPS results, the constant photocatalytic performance and the unaltered thin film morphology after the stearic acid degradation test confirmed the stability of the B-TiO₂ thin film. Several cycles of cleaning and UV irradiation did not involve the loss of boron. This stability is due to the interstitial occupancy of boron in the TiO₂ lattice, fact which has been reported and studied previously by N. Patel *et al.*²⁵

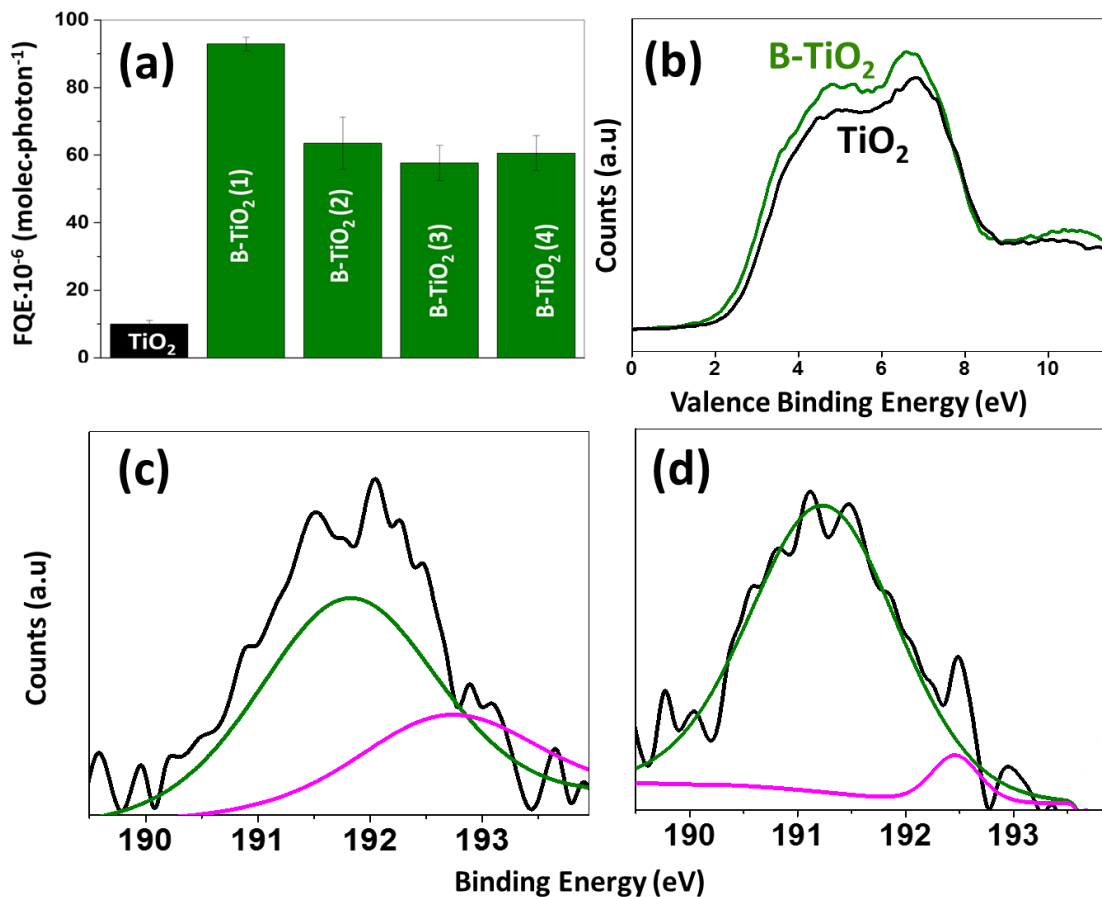


Figure 4. (a) Formal quantum efficiencies (FQE) obtained during photodegradation of stearic acid under UV irradiation of B-TiO₂, repeated four times (four runs) and average FQE of different undoped TiO₂ films, synthesised in the same conditions; (b) Valence Band XPS spectrum of B-TiO₂ and undoped TiO₂; and XPS spectra (c & d) after the second and third run of the photocatalytic test, respectively.

In conclusion, a new facile strategy to synthesise and deposit interstitial boron-doped TiO₂ transparent thin films using atmospheric pressure chemical vapour deposition (APCVD) has been presented. Analysis by XRD, Raman, XPS, SEM and photocatalytic measurements highlighted the benefit of interstitial boron-doping on the crystallite size and photocatalytic

properties of the films. The interstitial boron-doping of APCVD TiO₂ thin films may also positively affect other functional properties of the films and further work is currently being carried out to explore more possible functional properties of this new material, including an extension of the photocatalytic activity to the visible range of solar spectrum and more optical and electrical properties. Interstitial B-TiO₂ thin films might be also useful for a wide range of applications, such as antibacterial coating, self-cleaning materials, photoelectrochemical cells for solar energy harvesting devices, water splitting, etc.

ASSOCIATED CONTENT

Supporting Information. Further experimental details, schematic representation of the APCVD apparatus, cross-section SEM and zoomed top view of B-TiO₂ film, O 1s, Ti 2p and B 1s after thermal treatment XPS spectra of the B-TiO₂ film, IR spectra of stearic acid degradation when testing photocatalysis, SEM image of the B-TiO₂ film after the photocatalytic test and Tauc plot of the undoped and B-TiO₂. This material is available free of charge via the Internet at <http://pubs.acs.org>.

AUTHOR INFORMATION

Corresponding Author

* E-mail: i.p.parkin@ucl.ac.uk

Author Contributions

The manuscript was written through contributions of all authors. All authors have given approval to the final version of the manuscript.

Funding Sources

Miguel Q.-G., and Nicolas D. B. are grateful to the Luxembourgish “Fonds National de la Recherche” (FNR) for financial support through the PlasmOnWire project.

Notes

The authors declare no competing financial interest.

ACKNOWLEDGMENT

Mr. Carlos Sotelo-Vazquez, Dr. Raúl Quesada-Cabrera and Dr. Andreas Kafizas are thanked for useful discussions. Dr. Steven Firth and Dr. Robert Palgrave are also thanked for access and assistance to the SEM, Raman and XPS instruments.

REFERENCES

- (1) Hu, S.; Shaner, M. R.; Beardslee, J. A.; Lichterman, M.; Brunschwig, B. S.; Lewis, N. S. Amorphous TiO₂ Coatings Stabilize Si, GaAs, and GaP Photoanodes for Efficient Water Oxidation. *Science*. **2014**, *344*, 1005–1009.
- (2) Kafizas, A.; Parkin, I. P. Inorganic Thin-Film Combinatorial Studies for Rapidly Optimising Functional Properties. *Chem. Soc. Rev.* **2012**, 738–781.
- (3) Kafizas, A.; Kellici, S.; Darr, J. A.; Parkin, I. P. Titanium Dioxide and Composite Metal/metal Oxide Titania Thin Films on Glass: A Comparative Study of Photocatalytic Activity. *J. Photochem. Photobiol. A Chem.* **2009**, *204*, 183–190.
- (4) Page, K.; Palgrave, R. G.; Parkin, I. P.; Wilson, M.; Savin, S. L. P.; Chadwick, A. V. Titania and Silver–titania Composite Films on Glass—potent Antimicrobial Coatings. *R. Soc. Chem.* **2006**, *17*, 95–104.
- (5) Mills, A.; Crow, M.; Wang, J.; Parkin, I. P.; Boscher, N. Photocatalytic Oxidation of Deposited Sulfur and Gaseous Sulfur Dioxide by TiO₂ Films. *J. Phys. Chem. C* **2007**, *111* (14), 5520–5525.

- (6) Liu, B.; Aydil, E. S. Growth of Oriented Single-Crystalline Rutile TiO₂ Nanorods on Transparent Conducting Substrates for Dye-Sensitized Solar Cells. *J. Am. Chem. Soc.* **2009**, *131*, 3985–3990.
- (7) Mills, A.; Le Hunte, S. An Overview of Semiconductor Photocatalysis. *J. Photochem. Photobiol. A Chem.* **1997**, *108*, 1–35.
- (8) Henderson, M. A. A Surface Science Perspective on TiO₂ Photocatalysis. *Surf. Sci. Rep.* **2011**, *66*, 185–297.
- (9) <http://www.nsg.com/>.
- (10) Velten, D.; Biehl, V.; Aubertin, F.; Valeske, B.; Possart, W.; Breme, J. Preparation of TiO₂ Layers on Cp-Ti and Ti6Al4V by Thermal and Anodic Oxidation and by Sol-Gel Coating Techniques and Their Characterization. *J. Biomed. Mater. Res.* **2002**, *59*, 18–28.
- (11) Carlsson, J. Chemical Vapor Deposition. *Handb. Depos. Technol. Film. Coatings* **2010**, 400–459.
- (12) Zaleska, A. Doped-TiO₂: A Review. *Recent Patents Eng.* **2008**, *2*, 157-164 **2008**, No. 1, 157–164.
- (13) Guillot, J.; Lecoq, E.; Duday, D.; Puhakka, E.; Riihimäki, M.; Keiski, R.; Chemin, J.-B.; Choquet, P. Combining a Molecular Modelling Approach with Direct Current and High Power Impulse Magnetron Sputtering to Develop New TiO₂ Thin Films for Antifouling Applications. *Appl. Surf. Sci.* **2015**, *333*, 186–193.
- (14) Burda, C.; Chen, X.; Narayanan, R.; El-Sayed, M. A. Chemistry and Properties of Nanocrystals of Different Shapes. *Chemical Reviews.* **2005**, *105*, 1025–1102.
- (15) O'Neill, S. A.; Parkin, I. P.; Clark, R. J. H.; Mills, A.; Elliott, N. Atmospheric Pressure Chemical Vapour Deposition of Titanium Dioxide Coatings on Glass. *J. Mater. Chem.* **2002**, *13*, 56–60.

- (16) Tseng, T. K.; Lin, Y. S.; Chen, Y. J.; Chu, H. A Review of Photocatalysts Prepared by Sol-Gel Method for VOCs Removal. *Int. J. Mol. Sci.* **2010**, *11*, 2336–2361.
- (17) Choy, K. Chemical Vapour Deposition of Coatings. *Prog. Mater. Sci.* **2003**, *48*, 57–170.
- (18) Scanlon, D. O.; Dunnill, C. W.; Buckeridge, J.; Shevlin, S. A.; Logsdail, A. J.; Woodley, S. M.; Catlow, C. R. A.; Powell, M. J.; Palgrave, R. G.; Parkin, I. P.; Watson, G. W.; Keal, T. W.; Sherwood, P.; Walsh, A.; Sokol, A. A. Band Alignment of Rutile and Anatase TiO₂. *Nat. Mater.* **2013**, *12*, 798–801.
- (19) Palgrave, R. G.; Parkin, I. P. Aerosol Assisted Chemical Vapor Deposition Using Nanoparticle Precursors: A Route to Nanocomposite Thin Films. *J. Am. Chem. Soc.* **2006**, *128*, 1587–1597.
- (20) Asahi, R.; Mikawa, T.; Ohwaki, T.; Aoki, K.; Taga, Y. Visible Light Photocatalysis in Nitrogen-Doped Titanium Oxides. *Science*. **2001**, *293*, 269–271.
- (21) Quesada-Cabrera, R.; Sotelo-Vazquez, C.; Darr, J. A.; Parkin, I. P. Critical Influence of Surface Nitrogen Species on the Activity of N-Doped TiO₂ Thin-Films during Photodegradation of Stearic Acid under UV Light Irradiation. *Appl. Catal. B Environ.* **2014**, *160*, 582–588.
- (22) Xu, T.-H.; Song, C.-L.; Liu, Y.; Han, G.-R. Band Structures of TiO₂ Doped with N, C and B. *J. Zhejiang Univ. Sci. B* **2006**, *7*, 299–303.
- (23) Yang, K.; Dai, Y.; Huang, B. Origin of the Photoactivity in Boron-Doped Anatase and Rutile TiO₂ Calculated from First Principles. *Phys. Rev. B - Condens. Matter Mater. Phys.* **2007**, *76*, 1–6.
- (24) Zaleska, A.; Grabowska, E.; Sobczak, J. W.; Gazda, M.; Hupka, J. Photocatalytic Activity of Boron-Modified TiO₂ under Visible Light: The Effect of Boron Content, Calcination Temperature and TiO₂ Matrix. *Appl. Catal. B Environ.* **2009**, *89*, 469–475.

- (25) Patel, N.; Dashora, A.; Jaiswal, R.; Fernandes, R.; Yadav, M.; Kothari, D. C.; Ahuja, B. L.; Miotello, a. Experimental and Theoretical Investigations on the Activity and Stability of Substitutional and Interstitial Boron in TiO₂ Photocatalyst. *J. Phys. Chem. C* **2015**, *119*, 18581–18590.
- (26) Carmichael, P.; Hazafy, D.; Bhachu, D. S.; Mills, A.; Darr, J. A.; Parkin, I. P. Atmospheric Pressure Chemical Vapour Deposition of Boron Doped Titanium Dioxide for Photocatalytic Water Reduction and Oxidation. *Phys. Chem. Chem. Phys.* **2013**, *15*, 16788–16794.
- (27) Slink, W. Vanadium-Titanium Oxide Catalysts for Oxidation of Butene to Acetic Acid. *J. Catal.* **1981**, *68*, 423–432.
- (28) Artiglia, L.; Lazzari, D.; Agnoli, S.; Rizzi, G. A.; Granozzi, G. Searching for the Formation of Ti – B Bonds in B - Doped TiO₂ – Rutile. *J. Phys. Chem. C*, **2013**, *2*, 13163-13172.
- (29) Mills, A.; Wang, J. Simultaneous Monitoring of the Destruction of Stearic Acid and Generation of Carbon Dioxide by Self-Cleaning Semiconductor Photocatalytic Films. *J. Photochem. Photobiol. A Chem.* **2006**, *182*, 181–186.